Atmospheric Corrosion Kinetics and Dynamics of Karachi Onshore Areas

[1]Mazher Islam Khan, [1]Humaira Bano, [2]Hamida Tabassum Seema Khan, [3]Azhar Mahmood and [4]Syed Arif Kazmi*
[1]Department of Chemistry, University of Karachi, Karachi, Pakistan.
[2]DHA College for Women, Phase VIII, Karachi, Karachi, Pakistan.
[3]National University of Sciences and Technology, Islamabad, Pakistan.
[4]ICCBS HEJ Research Institute of Chemistry, University of Karachi, Karachi, Pakistan.
humairab@uok.edu.pk, kazmi_arif@yahoo.com

(Received on 29 September 2014, accepted in revised form)

Summary: Atmospheric corrosion kinetics and dynamics (rate and factors) of Karachi coastal city was ascertained at a couple of locations in the vicinity of Arabian seashore i.e. Hawksbay and Seaview Township by complying ISO 9223, ASTM G01 and ASTM G50 norms. Both exposure test sites were located at west to south-westward wind corridor. Data was collected for exposure of mild steel coupons at these two locations and their meteorological conditions were logged for a period from March 2005 to April 2007. Chloride and Sulfur dioxide were measured by employing ISO 9225 standard. Severe degree of material depletion for mild steel coupons was observed at both test locations. Mass loss was higher at Hawksbay test site than at Sea view Township. Maximum mass loss was observed during monsoon period probably due to rainfall and strong sea wave action which produced enriched marine aerosols and boosted chloride deposition rates. Although paucity of rainfall was observed but substantial relative humidity level was recorded during test period. Comparison of the results indicated that corrosion rate was higher at Hawksbay test site as compared to Seaview test site. Goethite and lepidocrocite were identified as major corrosion products by Scanning electron microscopy while it was also revealed that major portion of lepidocrocite phase was transformed into goethite at Seaview test site. As goethite phase is thermodynamically more stable and less vulnerable to further recurrence of corrosion as compared to lepidocrocite phase which may be attributed to less corrosion rate measured at Seaview test site. Since corrosion rate at both locations were gauged in the range of $65 > r_{corr} \leq 150$ in terms of $\mu m.year^{-1}$ so this study ranked the corrosivity of these two test locations as C_5 i.e. very high marine corrosivity.

Key Words: Atmospheric corrosion, mild steel, marine corrosivity, scanning electron microscopy.

Introduction

The term corrosion is a derivative of Latin word 'corrosus' which stands for disintegrate away or deteriorate by degrees; an unpleasant term for an undesirable process [1]. Atmospheric corrosion is the most widespread type of corrosion for metal structures and accounts for gigantic damages both on basis of material and cost [2]. Atmospheric corrosion is a worldwide issue due to its significant effect on the operational life of machineries and on the permanence of engineering materials as colossal amount of materials are exposed and attacked by atmospheric pollutants. General atmospheric attributes that may induce corrosion, consist of meteorological parameters such as humidity, rain, temperature, sun rays, wind speed, etc. Atmospheric pollutants like SO_2, H_2S, Cl^- and oxides of nitrogen, have also played their role in atmospheric corrosion [3-4]. Although there is a comprehension about various kinds of conventional parameters that may induce corrosion but these general agreements setback adversely due to their extremely poor predictability because of diversity and complex nature of the atmosphere. Therefore synergistic function of these parameters may be accounted in the calculation for acquiring a definite conclusion. A viable way out to this discrepancy is to gauge the pragmatic corrosion rates and the contributing atmospheric factors and then correlate them [5-6].

Corrosion deprivation may be about 4-5 % of a country GNP while atmospheric corrosion is a key contributor to these losses [7]. Structural engineers indispensably need corrosivity data and composition of atmospheric pollutants of a location for curtailing down corrosion losses [8]. Corrosion damages are generally confronted with other catastrophes such as seismic shocks and storms. However, in the case of seismic activity, mapping of seismic zones is formerly in vogue while in the case of storms, global weather forecast is also attainable but on other hand no global corrosivity map has been drawn up till now. Even various countries have individually drafted their corrosivity maps which restricted to the area of their concern. This modern era of global village and industrial revolution demands drafting of global corrosion maps and its periodic revision [9]. Many corrosion scientists have worked in corrosion field and contributed corrosion data of their region for global corrosion mapping [10-16].

Atmospheric corrosion is a severe hazard to all engineering structures, industrial installations and

*To whom all correspondence should be addressed.

civil construction setting up near Karachi's coastal line. An immense deterioration has been observed in the last three decades which in turn increased repairing needs of coastal area installations. Notwithstanding, up till now no comprehensive atmospheric corrosion relevant study has been executed for Karachi coastal areas. Therefore it is need of hour to conduct corrosion study of Karachi city on scientific basis to ascertain the kinetics and dynamics (rate and factor) of corrosive attack, in order to arrive at a definite solution. Subject study was conducted for a period of 25 months i.e. March 2005 to April 2007 to conceive abovementioned objective. Moreover, this communication would also contribute corrosivity data of Karachi city for global corrosivity mapping.

Experimental

Selection of Atmospheric Exposure Test Sites

Karachi metropolitan city is spread over approximately 60 Km long coastal line, starting from DHA Phase VIII to Ras Muari (Cape Monze). Exposure test sites selection was based on various criterions like wind direction, source of pollution, distance from sea shore etc. While accounting these criteria it was ascertained that the corrosion rate would be much higher in the coastal areas which are situated along west and south westerly wind direction. This wind direction remains from March till October. Furthermore, Karachi harbor engaged with shipment of various petroleum products, industrial raw supplies and synthetic products while SITE Industrial zone involved in emission of different chemical pollutants. Therefore, these two sites were believed to be main anthropogenic source of atmospheric pollution in Karachi city. For subject study two exposure test sites were selected across aforementioned anthropogenic sources and along west and south westerly wind corridor. These two sites included Seaview Township, DHA Phase VI and Hawksbay Beach which are distant apart about 25 Km. Geographical positioning of these two test sites are tabulated in Table-1. About two years field exposure test program (March 2005 to April 2007) was performed at these selected sites.

Table-1: Geographical Data of the Exposure Sites Located at Karachi Coastal Area.

Test Sites	Latitude	Longitude	Distance from Sea
Seaview Township	24° 47' 05.50'' N	67° 03' 08.18'' E	300 m
Hawksbay	24° 51' 36.56'' N	66° 51' 42.40'' E	100 m

Preparation of Test Coupons and Atmospheric Exposure Testing

ASTM G 50 norms were followed for the preparation of exposure rack and test coupons [17]. Exposure rack was made from wood. In order to hold the test coupons ceramic separators were fixed on the wooden frame with the help of stainless steel nuts. Mild steel sheet of 2.5 mm thickness was provided by Hino-Pak motors limited. Mild steel coupons of dimensions 103 mm x 152 mm (4` × 6`) in size were cut from the sheet. Trimming of the edges was carried out in order to make the edges smooth. A hole was made at the top of test coupons which was used later to tie the tags. Test coupons were thoroughly cleaned with degreasing solvents gasoline and acetone, wiped and finally dried. After drying, test coupons were weighed and results were recorded as mass of test coupons before exposure. Photographs of the test coupons were also taken before exposure. Prepared test coupons were mounted on wooden frames with ceramic separators at 45º angle and exposed at two selected exposure test sites of Karachi coastal area facing west-south west direction. Fig. 1 showed exposure of test panels at two exposure sites located at Karachi coastal area.



Fig. 1: Exposure Experiment of Test Panels (in progress) at Two Exposure Test Sites Located at Karachi Coastal Area (a) Hawksbay (b) Seaview.

Metallurgical composition of mild steel test coupons was determined by using optical emission spectroscopy. This facility was provided by Pakistan Steel mills. Metallurgical composition of mild steel test coupons were found to be Fe (99.77 %), C (0.029 %), Si (0.012 %), Mn (0.14 %), P (0.01 %), S (0.012 %), Ni (0.013 %) and Cr (0.015 %) in terms of weight percentage.

Gauging of Meteorological Parameters

Weather data was gauged for the entire exposure test period. Thermal conditions, wind velocity & direction, rainfall, dew point and relative humidity data were collected and verified by weather stations.

Measurement of Pollutants (Chloride and Sulfur dioxide)

Amount of chloride and sulfur dioxide was measured by complying method recommended by ISO 9225 [18]. According to this standard wet candle method was used for the determination of atmospheric chloride. A wooden assembly was prepared and installed with fixed conical flask. In this conical flask 350 ml of the reagent water was poured. Reagent water was prepared by mixing glycerin, octanoic acid and deionized water. For the preparation of candle, cotton gauze was wrapped on test tube and the wick ends of the gauze were inserted into flask and the stopper was fixed firmly in to the neck of the flask. The flask and the whole assembly were rinsed with reagent water to remove any contaminants. These candles were placed at the two selected test sites in order to collect the data related to chloride deposition. These candles were removed on monthly basis and deposited chloride was extracted from the candles. Finally the amount of chloride collected was measured by using Kitagawa pre calibrated tubes.

Sulfur dioxide was measured by dry panel method. For the preparation of sulfation plates, filter paper circles were bonded to the bottom of polystyrene petri dishes. Then acetone was squirted into the dish in order to saturate the filter paper. Filter paper was pressed firmly with a glass rod just to adhere it completely to the dish. Then acetone was allowed to evaporate. A uniform mixture was prepared by mixing powdered gum tragacanth and PbO_2. 10 ml of this mixture was carefully poured into dishes with the help of pipette. Prepared plates were kept in an oven set at 40 °C to 50 °C for 20 h and finally cooled. Now these sulfation plates were placed in a wooden assembly and exposed at the two exposure test sites. These sulfation plates were removed on monthly basis. Finally the amount of sulfur dioxide collected by this method was measured by using Kitagawa pre calibrated tubes.

Mass Loss Data

Mass loss data was measured in compliance with ISO 8407 method [19]. For this purpose, test coupons were removed from the wooden frames and wrapped in air tight plastic bags and brought to the laboratory after exposure period. Mass losses were recorded with sixty days interval. Corrosion product was removed by using a mixture of HCl with Sb_2O_3 and $SnCl_2$ and then thoroughly cleaned with de-ionized water and flushed with acetone. After drying, test coupons were weighed and results were recorded as mass of test coupons after exposure. Mass loss was calculated by taking difference of pre and post exposure test masses of sample coupons while mass loss temporal trend was plotted for the exposure time period.

Determination of Corrosion Rates

Corrosion rates in μm/year for the two exposure test sites were calculated with the help of following formula [20]:

$$\text{Corrosion rate} = K \times \left[\frac{\Delta W}{A \times D \times T}\right]$$

where, Corrosion rate is in μm/year, K = Constant and its value is 87,600 [20], ΔW = Mass loss in mg, A = Area in cm^2, D = Density in g/cm^3, T = Time of exposure in hours

Characterization of Corrosion Products

Scanning electron microscopy (SEM) technique was employed to study the morphology of the corrosion products [21]. Corrosion product formed on the surface of mild steel test coupons after one year exposure was taken. A small section of the corroded test coupon was taken and gold coating was carried out by a gold coater (JEOL JFC 1500) up to $300A^0$. Afterward samples were scanned by a Scanning electron microscope (JEOL 6380A) at operational conditions of 10^{-7} Torr vacuum and 15 kV.

Results and Discussion

Objective of this study was to ascertain corrosion rate (r_{corr}) and various meteorological parameters such as temperature (T), relative humidity

(RH) and atmospheric pollutants (Cl^- and SO_2) and correlate them. Moreover subject research was intended to establish corrosivity category of the Karachi coastal area atmospheres as per ISO 9223 standard which is function of three factors: corrosion rate (r_{corr}), air salinity (S) and SO_2 pollution (P). Scanning electron microscopy (SEM) technique was also employed to study the morphological configuration of corrosion products formed on exposed mild steel coupons.

Meteorological Parameters of Karachi Coastal Area

Environment of coastal areas are usually very much corrosive. Corrosivity of onshore atmosphere depends on the geography of the coast, tide influx at the shoreline, thermal conditions, precipitation (fog, rain, snow), winds (direction and speed) and moist conditions. Corrosivity drops sharply while moving away from the shore. Vigorous hurricane can spray salt up to 15 km at ground [22].

The Weather data measured during the exposure test period showed corrosion invigorating meteorological conditions during March to September of each exposure test year. During this period, the wind blows from sea to land in west and south-westward which carries corrosive sea aerosols (Table-2) while high wind speed also recorded during this epoch tentatively (Fig. 2). These salt-laden airs can induce very intense corrosive attack on several engineering materials, promote electrochemical corrosion and brings damage to coating materials. In Karachi, monsoon period extends from June to September of each year during which airborne marine aerosols carries high concentration of chlorides probably due to strong sea wave action which produced enriched marine aerosols and boost chloride deposition rates.

Atmospheric corrosion has a complex interaction with temperature variable. Generally hot conditions will enhance corrosiveness by accelerating the kinetics of galvanic reactions and by promoting mass diffusion processes [23]. Karachi enters in summer tentatively from May and in winter from November. Temporal temperature changes were logged and it was observed that May to July was warm period whereas average highest and lowest recorded temperatures were about 310 K and 304 K respectively. Therefore May and June remained hottest months whereas November to January was cold months (Fig. 3). During summer period atmospheric chemistry is vigorous due to high temperature which synergistically acts with other turbulent monsoon fickle climatic elements.

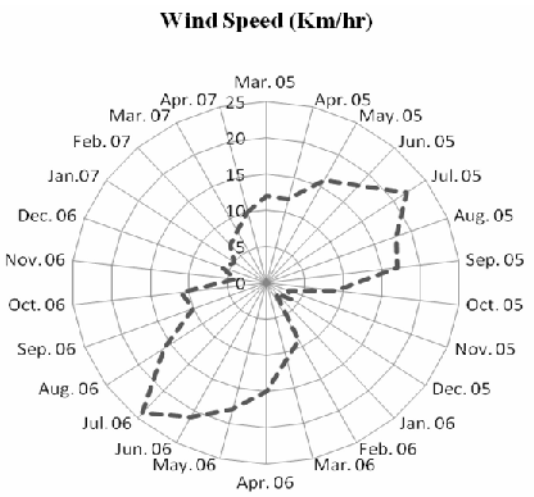

Fig. 2: Temporal Trend of Average Wind Speed at Karachi City during Exposure Experiment Time Period.

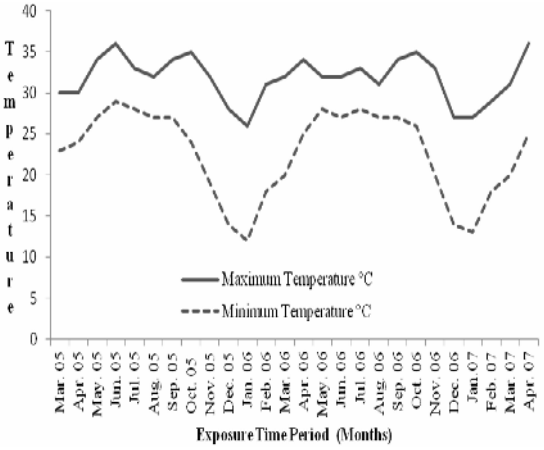

Fig. 3: Temporal Trend of Maximum and Minimum Average Temperature of Karachi City during Exposure Experiment Time Period.

A wet humidity layer is formed on structural surfaces by the adsorption of water droplets at a definite humidity level which mainly depends upon dew rate, ocean mist, rainfall, and other types of water splashing. In seashore environment, salt is carried upon structural surfaces by oceanic fog and windblown water sprays which accelerate corrosion due to its electrolytic stimulation at relative humidity more than 55 % [22]. At exposure test sites relative humidity marginally crossed this threshold limit during March to September (Fig. 4).

Table-2: Wind Direction Data of Karachi Coastal Area.

Month			Mar. 05	Apr. 05	May. 05	Jun. 05	Jul. 05	Aug. 05	Sep. 05	Oct. 05	Nov. 05	Dec. 05
Wind Direction			W	W	W/SW	W/SW	W	W/SW	W/SW/N	W/SW/N	W/S/E/N	E/NE/W
Degree			270	270	270-240	270-240	270	270-240	270-240-360	270-240-360	270-180-90-360	90-60-270
Month	Jan. 06	Feb. 06	Mar. 06	Apr. 06	May. 06	Jun. 06	Jul. 06	Aug. 06	Sep. 06	Oct. 06	Nov. 06	Dec. 06
Wind Direction	E NE W	W/NW/E	W/SW/E	W	W	W/SW	W/SW	W/SW	W	W/NW	W/E/N	E/NE/W
Degree	90-120-270	270-120-90	270-240-90	270	270	270-240	270-240	270-240	270	270-120	270-90-360	90-60-270
Month	Jan.07	Feb. 07	Mar. 07	Apr. 07								
Wind Direction	NE/W	W/NW/E	W/NW	W								
Degree	60-270	270-120-90	270-240	270								

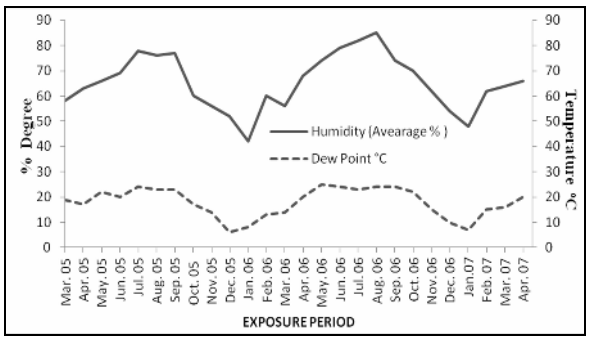

Fig. 4: Temporal Trend of Average Humidity and Dew Point of Karachi City during Exposure Experiment Time Period.

Irrespective to corrosion strong reliance on humidity level there is a comprehension that frequency, intensity and pH of rainfall are key factors that drive the corrosion kinetics [24]. Drizzling rain of season causes deposition of suspended particulate matters and salts on exposed faces of metallic structure developing metallic patina while heavy rains runoff these deposition and leave clear faces. In Karachi, rainy period usually commenced in June extend up to September. During year 2005 and 2006 maximum annual precipitation level was recorded up to 35 mm and 120 mm respectively (Fig. 5). Data plotted showed paucity of rainfall at Karachi city, caused deposition of suspended atmospheric pollutants and formation of damp moist layer but not enough to substantially runoff these deposition.

Atmospheric Corrodents/Pollutants (Chloride and Sulfur dioxide)

Corrosion kinetic is a function of atmospheric aggressiveness, which in turn build upon various meteorological and pollution parameters. In coastal environment chloride crystals are formed by evaporation of droplets sprayed by the sea breeze. Many authors from all over the world have reported that chloride ion is chief culprit in onshore corrosion. In ferrous alloys, both Cl^- and OH^- anions compete for Fe^{2+} cation which produced during anodic reaction. Resultant iron-chloride products are thermodynamically not stable and get dissolved hence further corrosion continued [25-27].

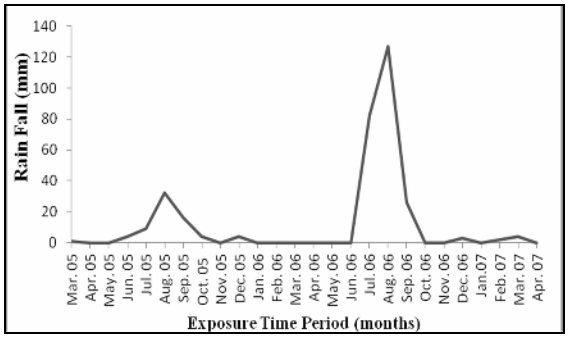

Fig. 5: Temporal Trend of Average Rainfall (mm) in Karachi City during Exposure Experiment Time Period.

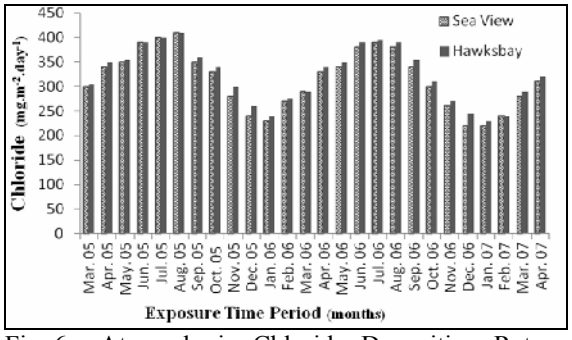

Fig. 6: Atmospheric Chloride Deposition Rate as Determined by Wet Candle Method at the Two Test Sites of Karachi City during Exposure Experiment Time Period.

Salinity measured at both test sites showed that chloride concentration was much higher in summer time during the monsoon period when wave action was stronger, this period was from late June till early September (Fig. 6). Chloride deposition rate measured during exposure period at both test sites varied between 220 mg/m^2.day to 300 mg/m^2.day in

winter and 340 mg/m^2.day to 405 mg/m^2.day during summer. So according to ISO/DIS 9223 the atmospheric salinity pollution classification in terms of deposition of chloride is S_2 ($60 < S_2 \leq 300$) in winter and S_3 ($300 < S_3 \leq 1500$) in summer for both test sites.

Major anthropogenic source of SO_x pollution is the ignition of hydrocarbon fuels comprising sulfur which released most of sulfur in the form of SO_2 gases. This is well established fact that SO_2 gases in atmosphere significantly promote the metal corrosion [28]. Rozenfeld has proposed that reduction of SO_2 may be preferably faster than O_2 at cathodic sites due to its higher solubility ($SO_2 > O_2 \times 2600$), as a result accelerating metal dissolution rates at anode [29].

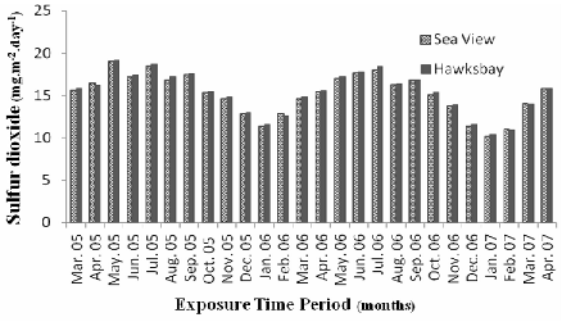

Fig. 7: Atmospheric Sulfur Dioxide Deposition Rate as Determined by Dry Panel Method at the Two Test Sites of Karachi City during Exposure Experiment Time Period.

As far as sulfur dioxide is concerned, results clearly indicate that there was a temporal variation in sulfur dioxide deposition rate during the exposure time period at both exposure sites (Fig. 7). Concentration of sulfur dioxide was higher (15-19 mg/m^2.day) from April to October and lower (11-16 mg/m^2.day) from November to February. So according to ISO/DIS 9223 the atmosphere classification category in terms of deposition of sulfur dioxide is P_1 ($10 < P_1 \leq 35$) for both test sites.

Comparison of the results with previous studies at sub continent region showed that average values of deposition of chloride and sulfur dioxide at both test sites were very close to the values reported by M. Natesan et al, for the marine test site of Chennai, India [30].

Thus the classification of corrosivity based on atmospheric corrodents (chloride and sulfur dioxide) according to ISO 9224 was rated to be C_5 for both test sites [31].

Mass Loss and Corrosion Rates at Two Exposure Test Sites of Karachi Coastal Area

Pre and post exposure test condition of mild steel panels at both test sites of Karachi coastal area were snapped as Fig. 8. Comparison of their conditions corroborated that test coupons exposed at Hawksbay test site have suffered by more severe corrosion invasion and were completely deteriorated.

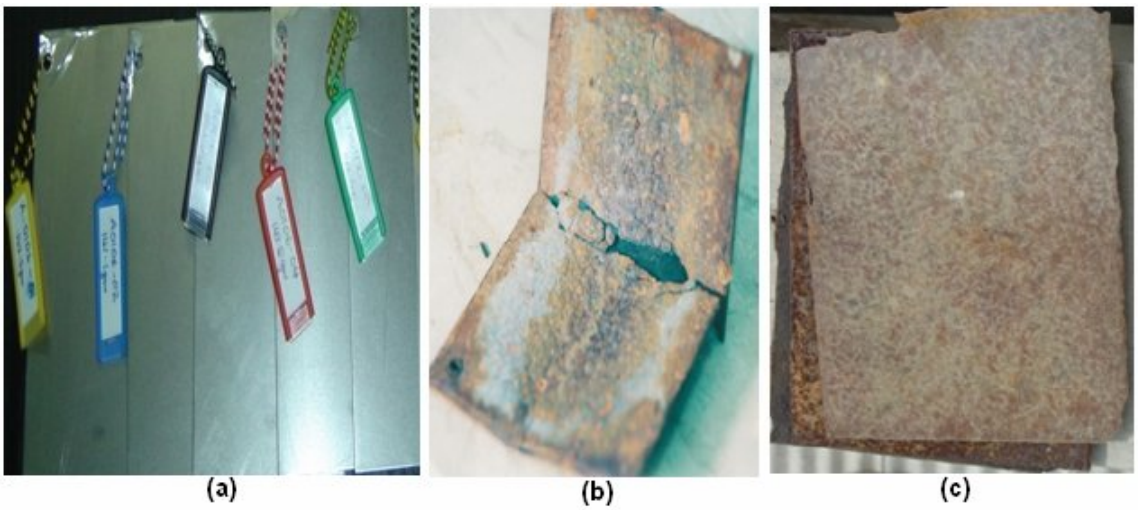

Fig. 8: Condition of Test Panels Exposed at Two Test Sites Located at Karachi Coastal Area (a) Before Exposure (b) After 2 Year Exposure at Hawksbay Test Site (c) After 2 Year Exposure at Seaview Test Site.

Seasonal trends of mass loss of test specimens at two exposure test sites were depicted in Fig. 9. Highest mass loss at both test sites was observed during July to August 2005 whereas the mass loss in the same period in the year 2006 was 10-15 % less. This could be due to lower rainfall in the year 2005 as compared to 2006. It was observed that the mass loss was higher at Hawksbay test site as compared to Seaview test site. This variation could be because of dissimilarity in position from the sea shore as Hawksbay test site was located comparatively closer to sea shore.

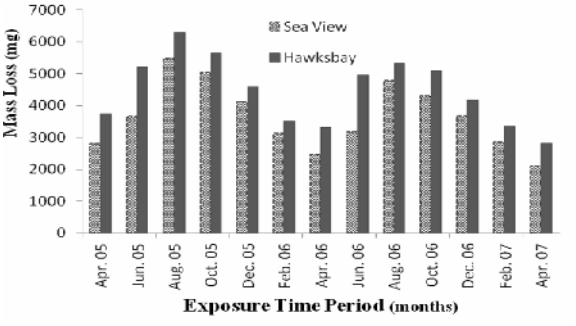

Fig. 9: Seasonal Trends in Mass Losses at Two Test Sites of Karachi City during Exposure Experiment Time Period.

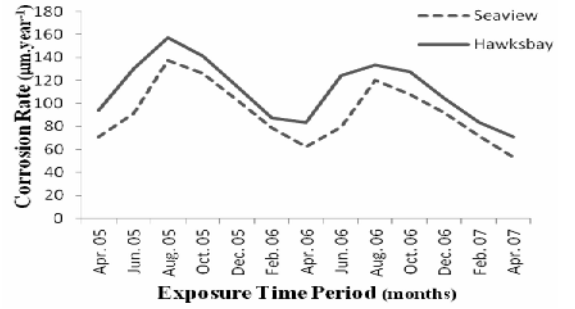

Fig. 10: Seasonal Trends in Corrosion rates at Two Test Sites of Karachi City during Exposure Experiment Time Period.

Mass loss method was adopted for measuring corrosion rates. Monthly corrosion rates were in full agreement with atmospheric aggressiveness established by the relative humidity, temperature and salinity values. Panels exposed in winter months (November to January) and summer months (May and June) suffered lower mass loss rather than that exposed in rainy months (July and August). Therefore seasonal corrosion rate of mild steel coupons was higher (137 µm.year^{-1}) in the rainy months in contrast to the corrosion rate in winter months (103.8 µm.year^{-1}) and in summer months (106.3 µm.year^{-1}) (Fig. 10). This is because of protective corrosion product film runoff frequently by rain unveiling underlying metal faces for further corrosion attack. As corrosion rate for both locations were calculated in the range of 65> $r_{corr} \leq 150$ µm.year^{-1} therefore this study appraised the corrosivity level of these two locations up to 'C_5' i.e. very high marine [32].

According to ISO 9223 standard, environmental data or corrosion rates values obtained after exposure can be used for the determination of corrosivity category [32]. Present study revealed that the corrosivity category obtained according to the environmental parameters is in full agreement with the corrosion rate data obtained for the Hawksbay and Seaview test sites located at Karachi coast.

Many researchers have carried out studies related to the determination of corrosion rates of mild steel exposed in marine environment [33-35]. Table-3 showed comparison of corrosion rate of mild steel exposed in marine environment with respect to different countries and sites. Results obtained from present study were also included in the Table-3. Comparison of the results with the reported data showed that the corrosion rate obtained at the two test sites of Karachi coastal area that is Hawksbay and Seaview are somewhat compatible with the values reported worldwide. It was also found that corrosion rates were lower than that observed in locations with similar chloride and sulfur dioxide deposition. Average values of deposition of chloride and sulfur dioxide at both test sites were very close to the values reported by M. Natesan et al, for the marine test site of Chennai, India [30]. But the corrosion rate at Chennai, India was higher than the corrosion rates obtained for both test sites in this study. On the other hand corrosion rate values of the present study are close to the value reported for Barranquilla, Colombia [35]. Although the deposition of chloride and sulfur dioxide at Barranquilla, Colombia was lower than obtained in this study. This is probably because of the reason that corrosion rate is influenced by a number of factors like geography of the coast, tide influx at the shoreline, thermal conditions, precipitation (fog, rain, snow), winds (direction and speed) and moist conditions [22].

Characterization of Corrosion Products

Corrosion kinetics are chiefly driven by properties of corrosion products which in turn mainly depends upon type of corrosive attack therefore corrosion products data may indeed proved helpful for incorporation of corrosion resistance in materials. Hindrance of corrosion products lamina lean on its density, expansion, fragility, homogeneity, permeability, inertness, adhesiveness and other properties whereas it considerably control corrosion kinetics and mechanisms through various

morphological structures. Corrosion products once duly formed and adhere in layers, mitigate the function of meteorological and pollution fickle elements [36]. Fig. 11 showed the scanning electron micrographs representing the morphology of the corrosion products after one year of exposure formed on the surface of mild steel coupons exposed at Hawksbay test site. These images indicated the presence of cotton ball like structure of goethite (α-FeO(OH)) and sandy crystals flowery structure of lepidocrocite (γ-FeO(OH)) in the corrosion product.

Fig. 12 showed the scanning electron micrographs representing the morphology of the corrosion products after one year of exposure formed on the surface of mild steel coupons exposed at Seaview test site. These images specified the presence of cotton ball like structure of goethite (α-FeO(OH)), flowery structure of goethite and flowery structure of lepidocrocite (γ-FeO(OH)) in the corrosion product.

Comparison of the results indicated that magnetite was not detected in the corrosion products of both test sites. It was also observed that goethite (α- FeO(OH)) was the main component in the corrosion product of Seaview test site while highly intermittent and open structure of lepidocrocite (γ-FeO(OH)) was noticed in the corrosion product of Hawksbay test site. Present study agreed well with the findings of other researchers who had identified these two components in the corrosion products formed in marine atmospheres [35].

Studies related to the characterization of corrosion products formed in atmospheric conditions have been reported by several authors [37-39]. According to the literature, rusts generated on the iron in the environment is because of electrochemical reactions. This rust is porous in nature due to which oxygen and water easily penetrates from the environment into the metal and exaggerates the corrosion.

$$2H_2O + O_2 + 4e^- \longrightarrow 4OH^- \quad (1)$$

$$Fe \longrightarrow Fe^{2+} + 2e^- \quad (2)$$

$$Fe^{2+} + 2OH^- \longrightarrow Fe(OH)_2 \quad (3)$$

$$Fe(OH)_2 + O_2 \longrightarrow Fe_2O_3.H_2O \text{ or } 2FeOOH \quad (4)$$

Table-3: Comparison of Corrosion Data Measured in Subject Study with Previous Studies Reported in Literature [33-35].

Country	Site	Steel Corrosion Rate µm.year^{-1}	Classification of Corrosivity As per ISO 9223	Cl^- Deposition mg/m^2.day	SO_2 Deposition mg/m^2.day
Pakistan (Current Study)	Hawksbay	157.5*	C_5	230 - 410†	19.2‡
	Seaview	137.3*	C_5	220 - 410†	18.5‡
Saudi Arabia	Frasan	279.27	C_5	ND	ND
	Jeddah	89	C_5	160	8.1063
	Yanbu	81.56	C_5	128	7.381
	Wajah	472.19	C_5	608	8.1059
Colombia	Barranquilla	168.67	C_5	96.59	5.16
India	Chennai	524	C_5	304.6	18
	Mangalore	108.4	C_5	69	Traces
	Manali	111.5	C_5	75.21	25

*Maximum value of corrosion rate, †RANGE of chloride deposited,
‡Maximum value of SO_2 deposition ND = Not determined

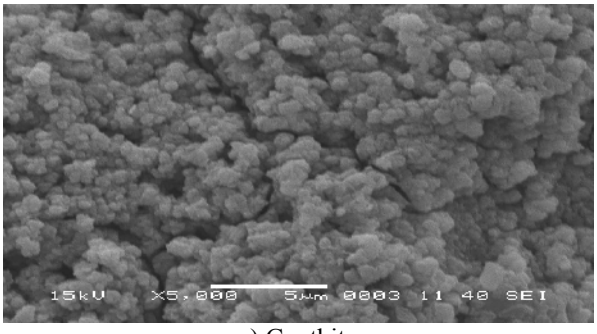

a) Geothite

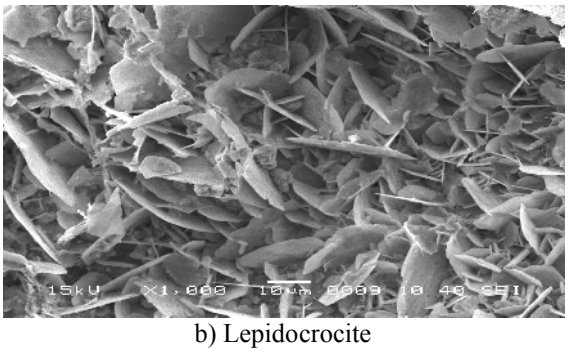

b) Lepidocrocite

Fig. 11: Scanning Electron Micrographs Showing the Morphology of the Corrosion Products Formed after one Year Exposure at Hawksbay Test Site (a) Ball like structure of Geothite (b) Flowery Lepidocrocite.

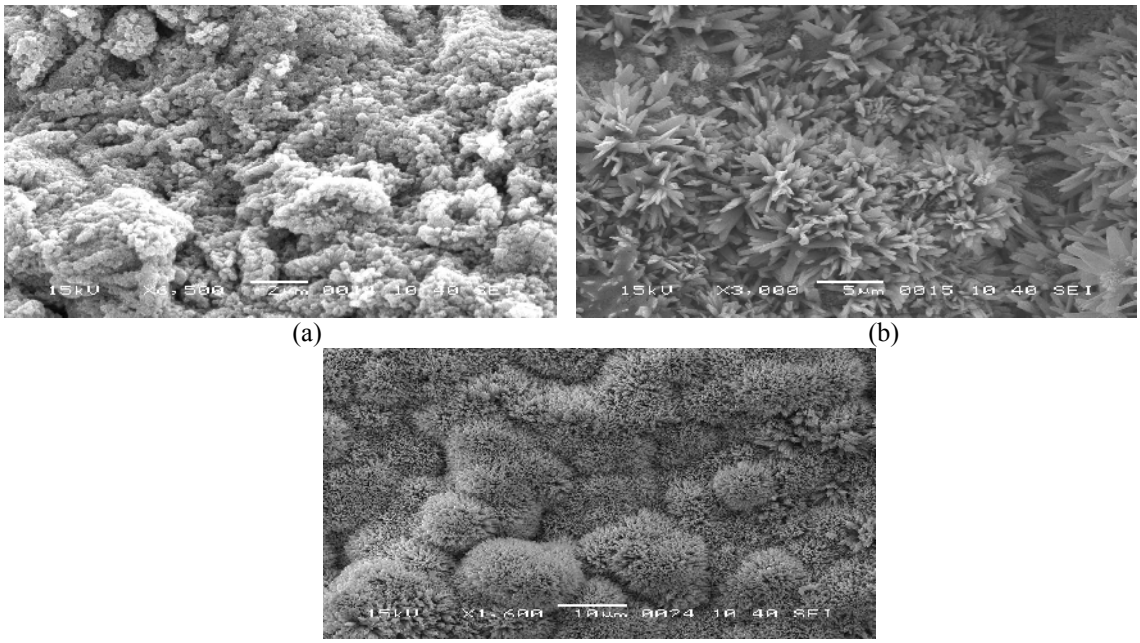

(a) (b)

(c)

Fig. 12: Scanning Electron Micrographs Showing the Morphology of the Corrosion Products Formed after one Year Exposure at Seaview Test Site (a) Cotton ball like structure of Geothite (b) Flowery lepidocrocite (c) Flowery structure of Geothite.

In the humid environment iron is first corroded to unstable rust lepidocrocite (γ-FeOOH), then with the interaction of water and oxygen γ-FeOOH partly or entirely transformed into stable rust goethite (α- FeOOH) [21]. Present study showed that on Seaview test site major portion of lepidocrocite was transformed into goethite. These two forms of rust influence the process of corrosion. Thermodynamically goethite is stable than lepidocrocite [21]. SEM images also indicated the compact nature of goethite which can efficiently avoid further interaction of oxygen, moisture and polluted gases with the mild steel. It means that goethite behave as a non-reactive corrosion product and ultimately protect the underlying metal from more corrosion. SEM images showed loose flowery structure of Lepidocrocite. Porosity of the structure is responsible for the transportation and storage of water, oxygen, electrolyte and pollutants. These pollutants particularly SO_2 and NO_2 lower the pH and accelerate the dissolution of lepidocrocite as a result concentration of Fe^{3+} increases which in turn causes further oxidation of iron because of its oxidation ability.

$$\gamma\text{-FeOOH} + 3H^+ \longrightarrow Fe^{3+} + 2H_2O$$

Thus lepidocrocite is more harmful kind of rust which causes recurrence of the abovementioned (eq 1- 4) corrosion reactions [21]. Hence the high corrosion rate at Hawksbay test site is attributed and well justified by the detection of lepidocrocite as main corrosion product.

Conclusions

The corrosivity category is a technical attribute of operational environment which is very helpful in material selection and to determine preventive action compatible to working conditions [22]. ISO 9223 standard permits the estimation of atmospheric corrosivity category as a derivative of the meteorological parameters and corrosion rate values [32]. In general, meteorological conditions of Karachi onshore areas were found to be severely aggressive which may be due to its location, topography, wind direction and not enough rainfall.

Atmospheric level of chloride and sulfur dioxide at both test sites were found to be S_2/S_3 and P_1 respectively as per ISO 9223 norm. Therefore classification of corrosivity based on atmospheric corrodents (chloride and sulfur dioxide) was ranked to be C_5 for both test sites. The classification of corrosivity based on corrosion rates measured by weight loss experiment at both test sites was also found to be C_5 according to ISO 9223 which was in full agreement with abovementioned atmospheric corrosiveness results. Comparison of the results indicated that corrosion rate was higher at Hawksbay test site as compared to Seaview test site.

Scanning electron microscopy showed that the most abundant constituent in corrosion products of mild steel for both test sites were goethite and lepidocrocite. It was also found that on Seaview test site major portion of lepidocrocite was transformed into goethite. These two forms of rust influence the process of corrosion. Thermodynamically goethite is stable than lepidocrocite. Thus lepidocrocite is more harmful kind of rust which causes recurrence of the corrosion reactions. Hence the high corrosion rate at Hawksbay test site is attributed and well justified by the detection of lepidocrocite as main corrosion product.

Therefore, subject study recommend the use of corrosion resistant materials for fabrication of structures, application of robust paint formulation and employment of stringent corrosion control methods for preservation of installation located at Karachi onshore areas.

Acknowledgment

Authors would like to acknowledge Dr. Sami-Uz-Zaman (a renowned environmentalist) Chairman of Global Environmental Lab, for his guidance and support during course of subject study. The authors would like to thanks M. Yousuf, Afshan Irfan and Sahar Kamal for their valuable input in analyzing samples using SEM facility in the Centralized Science Laboratories, University of Karachi, Pakistan. Acknowledgment is due to Dean Faculty of Science, University of Karachi, Pakistan for financial assistance. Authors have no conflict of interest.

References

1. T. C. E. Trimgham, *Causes and Prevention of Corrosion in AIR Craft*, SIR ISAAC, Pitman & Sons Ltd, London, p. 134 (1958).
2. P. C. Vasant and G. K. Bansal, A Study on Impact of Atmospheric Corrosion on Different Types of Metals, *Int. J. Chem. Sci. App.,* **4**, 7 (2013).
3. P. W. Brown and L.W. Masters, *Atmospheric Corrosion*, Wiley, New York, p. 89 (1982).
4. S. Syed, Atmospheric Corrosion of Hot and Cold Rolled Carbon Steel under Field Exposure in Saudi Arabia, *Corr. Sci.*, **50**, 1779 (2008).
5. X. Naixin, L. Zhao, C. Ding, C. Zhang, R. Li and Q. Zhong, Laboratory Observation of Dew Formation at an Early Stage of Atmospheric Corrosion of Metals, *Corr. Sci.*, **44**, 163 (2002).
6. J. C. Scully, *The Fundamentals of Corrosion*, Pergamon Press, New York, p. 232 (1990).
7. S. A. Bradford, *Corrosion Control*, CASTI publishing Inc, Alberta, Canada, p. 169 (2001).
8. P. S. Mohan, M. Natesan, M. Sundaram and K. Balakrishnan, *Atmospheric Corrosion at Different Locations in South India, Bull. Electrochem.*, **12**, 91 (1996).
9. M. Natesan, N. Palaniswamy, N. S. Rengaswamy, K. S. Rajesh and M. Raghavan, *7th. International Symposium on Advances in Electrochemical Science & Technology*, Chennai, India, (2002).
10. M. Natesan, G. Venkatachari, and N. Palaniswamy, Corrosivity and Durability Maps of India, *Corr. Prevent. Contr.*, **1**, 43 (2005).
11. M. Morcillo, B. Chico, D. D. L. Fuente, E. Almeida, G. Joseph, S. Rivero and B.Rosales, Atmospheric corrosion of reference metals in Antarctic sites, *Cold Regions Science and Technology*, **40**, 165 (2004).
12. F. Corvo, T. Perez, L. R. Dzib, Y. Martin, A. Castañeda, E. Gonzalez and J. Perez, Outdoor–Indoor Corrosion of Metals in Tropical Coastal Atmospheres, *Corr. Sci.*, **50**, 220 (2008).
13. L. T. H. Lien, P. T. San and H. L. Hong, Results of Studying Atmospheric Corrosion in Vietnam 1995–2005, *Sci. Technol. Adv. Mater.*, **8**, 552 (2007).
14. F. Karaca, Mapping the Corrosion Impact of Air Pollution on the Historical Peninsula of Istanbul, *J. Cult. Herit.*, **14**, 129 (2013).
15. J. Tidblad, Atmospheric Corrosion of Metals in 2010–2039 and 2070–2099, *Atmos. Environ.*, **55**, 1 (2012).
16. F. Corvo, C. Haces, N. Betancourt, L. Maldonado, L. Véleva, M. Echeverria, O.T. De Rincón and A. Rincon, Atmospheric Corrosivity in the Caribbean Area, *Corr. Sci.*, **39**, 823 (1997).
17. ASTM G50-76, *Standard Practice for Conducting Atmospheric Corrosion Tests on Metals*, Philadelphia, USA (2003).
18. ISO 9225, *Corrosion of Metals and Alloys – Corrosivity of Atmospheres – Measurement of Pollution*, Geneva, Switzerland (1992).
19. ISO 8407, *Corrosion of Metals and Alloys – Removal of Corrosion Products from Corrosion Test Specimens*, Geneva, Switzerland (1991).
20. ISO 9226, *Corrosion of Metals and Alloys - Corrosivity of Atmospheres - Determination of Corrosion Rate of Standard Specimens for the Evaluation of Corrosivity*, Geneva, Switzerland (1992).
21. W. Zise, X. Chunchun, C. Xia and X. Ben, The Morphology, Phase Composition and Effect of Corrosion Product on Simulated Archaeological Iron, *Chin. J. Chem. Eng.*, **15**, 433 (2007).

22. S. Syed, Atmospheric Corrosion of Materials, *Emira. J. Eng. Res*., **11**, 1 (2006).
23. P. R. Roberge, *Handbook of Corrosion Engineering*, McGraw-Hill, USA, p. 58 (1999).
24. T. E. Graedel, Corrosion Mechanisms for Zinc Exposed to the Atmosphere*, J. Electrochem. Soc.*, **136**, 193 (1989).
25. K. Barton, *Protection against Atmospheric Corrosion*, John Wiley & Sons, London, p. 93 (1976).
26. S. Feliu, M. Morcillo and J. S. Feliu, the Prediction of Atmospheric Corrosion from Meteorological and Pollution Parameters—I. Annual Corrosion, *Corr. Sci.*, **34**, 403 (1993).
27. C. Arroyave, F. A. Lopez and M. Morcillo, The Early Atmospheric Corrosion Stages of Carbon Steel in Acidic Fogs, *Corr. Sci.*, **37**, 1751 (1995).
28. T. E. Graedel, Gildes Model Studies of Aqueous Chemistry. I. Formulation and Potential Applications of the Multi-Regime Model, *Corr. Sci.*, **38**, 2153 (1996).
29. I. L. Rozenfeld, *Proceedings of 1st International Congress on Metallic Corrosion*, Butterworth, London, p. 243 (1961).
30. M. Natesan, S. Palraj, G. Venkatachari and N. Palaniswamy, Atmospheric Corrosion of Engineering Materials at Two Exposure Sites in Chennai—A Comparative Study, *Corrosion.*, **62**, 883, (2006).
31. ISO 9224, *Corrosion of metals and alloys – Corrosivity of Atmospheres – Guiding Values for the Corrosivity Categories*, Geneva, Switzerland (1992).
32. ISO 9223, *Corrosion of Metals and Alloys – Corrosivity of Atmospheres - Classification*, Geneva, Switzerland (1992).
33. M. Natesan, G. Venkatachari and N. Palaniswamy, Kinetics of Atmospheric Corrosion of Mild Steel, Zinc, Galvanized Iron and Aluminium at 10 Exposure Stations in India, *Corr. Sci.*, **48**, 3584 (2006).
34. S. Syed, Atmospheric Corrosion of Hot and Cold Rolled carbon Steel under Field Exposure in Saudi Arabia, *Corr. Sci.*, **50**, 1779 (2008).
35. J. G. Castano, C. A. Botero, A. H. Restrepo, E. A. Agudelo, E. Correa and F. Echeverria, Atmospheric Corrosion of Carbon Steel in Colombia, *Corr. Sci.*, **52**, 216 (2010).
36. M. Yamashita, T. Shimizu, H. Konishi, J. Mizuki and H. Uchida, Structure and Protective Performance of Atmospheric Corrosion Product of Fe–Cr Alloy Film Analyzed by Mössbauer Spectroscopy and with Synchrotron Radiation X-Rays, *Corr. Sci.*, **45**, 381 (2003).
37. A. K. Neufeld and I.S. Cole, Using Fourier Transform Infrared Analysis to Detect Corrosion Products on the Surface of Metals Exposed to Atmospheric Conditions, *Corrosion*., **53**, 778 (1997).
38. Q. X. Li, Z. Y. Wang, W. Han and E. H. Han, Characterization of the Corrosion Products Formed on Carbon Steel in Qinghai Salt Lake Atmosphere, *Corrosion*., **63**, 640 (2007).
39. R. Balasubramaniam, On the Corrosion Resistance of the Delhi Iron Pillar, *Corr. Sci.*, **42**, 2103 (2000).